Probability Analysis of Submarine Slope Stability with Consideration of the Spatial Variability of Sediment Strength

Bin ZHU[(1)], Tetsuya HIRAISHI and Qing YANG[(1)]

(1) State Key Laboratory of Coastal and Offshore Engineering, Dalian University of Technology, China

Synopsis

With the development of ocean engineering, the stability evaluation of submarine slopes has become more essential for the problems relating the stability of submarine foundations and the safety of offshore structures. The properties of marine sediments vary spatially in nature, and because of the depositional processes and the effective overburden pressure, there is an increasing trend with depth for the undrained shear strength of marine clay. To consider the spatial variability of soil strength in the stability evaluation of submarine slopes, the random field method and the limit equilibrium method are integrated in our study. A novel response surface method is proposed based on the Gaussian process regression to reduce the number of calls for direct slope stability analysis in the Monte Carlo simulations. Then illustrative examples of an infinite clay slope model and a two-dimensional submarine slope model are analyzed, taking the spatial variability of soil strength into consideration. The computational burden of the analysis using the surrogate model is significantly reduced making the prediction of submarine landslides more efficient.

Keywords: submarine slope, reliability analysis, spatial variability, random field, response surface method, Monte Carlo simulation

1. Introduction

The stability evaluation of submarine slopes plays an important role in ocean engineering. The process of submarine landsides involves many uncertainties, and not all failure mechanisms are fully understood. Therefore, probabilistic methods have been proposed and applied to the stability evaluation of submarine slopes. For example, Yang et al. (2007) used several reliability methods such as first-order second moment (FOSM) method, point estimate method, and response surface method (RSM) for the stability evaluation of submarine slopes; Zhu et al. (2018) analyzed the stability of submarine slopes using RSM along with the advanced FOSM method. However, in these

studies using the traditional reliability methods, soil properties are just treated as random variables ignoring the spatial variability. It has been indicated that soil properties possess spatial variability for the reason of geological process and loading history (Phoon and Kulhawy, 1999).

In this study, the spatial variability of soil strength was taken into consideration in the evaluation of the stability of submarine slopes by integrating the random field method and limit equilibrium method (LEM). The spatial variability of the soil strength is described by means of stationary and non-stationary random fields simulated by the method of Karhunen-Loeve (K-L) expansion. A novel RSM is proposed based on the Gaussian process regression (GPR) to construct a

surrogate model for the direct slope stability analysis. Then the failure probability of the submarine slope is effectively obtained from Monte Carlo simulation (MCS) with the GPR-based surrogate model. Illustrative examples of an infinite clay slope model and a two-dimensional submarine slope model are analyzed. The computational burden of the MCS using the proposed method is significantly reduced, making the prediction of submarine landslides more efficient.

2. Random Field Simulation

In nature, soil properties vary from point to point over space as the result of geologic process. It is commonly recognized that marine sediments possess inherent spatial variability. The spatial characteristics are determined by the statistic parameters and the correlation structure. The correlation structure of the random field is described by autocorrelation functions, and the squared exponential autocorrelation function is the most commonly used, which is expressed in the two-dimensional space as:

$$\rho = \exp(-(\frac{x_1 - x_2}{l_h})^2 - (\frac{y_1 - y_2}{l_v})^2) \tag{1}$$

where l_h and l_v are the correlation lengths in the horizontal and vertical directions, respectively.

2.1 Karhunen-Loeve expansion

Some methods have been proposed for the simulation of random fields. Among these methods, K-L expansion is one of the most commonly used, which is a series-expansion method based on the spectral decomposition of the autocorrelation function of the soil properties. In most cases, soil shear strength is simulated by a stationary random field, which means that the average value and standard deviation of the shear strength are constant with depth. The stationary Gaussian random field with mean value μ and standard deviation σ can be expressed by the truncated K-L expansion as:

$$\tilde{H}(x,\theta) = \mu + \sum_{i=1}^{N} \sigma \sqrt{\lambda_i} f_i(x)\xi_i(\theta) \tag{2}$$

where $\xi_i(\theta)$ is a set of uncorrelated random variables with zero mean and unit standard deviation. The number N of truncated terms relies on the ratio of the correlation distance to the geometry size. Based on the fact that soil properties are expected to vary smoothly in the domain of interest, most of the uncertainties could be captured by only a few terms of the K-L expansion. λ_i and $f_i(x)$ in Eq. (2) are the eigenpairs of the autocorrelation function, which can be obtained by solving the homogeneous Fredholm integral equation of the second kind. For most autocorrelation functions, the numerical methods are used to obtain the eigenpairs.

2.2 Non-Gaussian Random Field

The distributions of soil properties are often taken as log-normal in the probability analysis to avoid negative values of parameters (Cho 2010). Lacasse and Nadim (1996) also indicated that the undrained shear strength of soil tends to obey a log-normal distribution. In the log-normal case, the standard deviation and mean value should firstly be normalized as follows:

$$\sigma' = \sqrt{\ln[1+(\sigma/\mu)^2]} \tag{3}$$

$$\mu' = \ln \mu - \sigma'^2 / 2 \tag{4}$$

The random field of the property with log-normal distribution is then obtained from the exponential of the Gaussian random field as

$$H'(x,\theta) = \exp(\mu' + \sum_{i=1}^{N} \sigma' \sqrt{\lambda_i} f_i(x)\xi_i(\theta)) \tag{5}$$

2.3 Non-stationary Random Field

Although the stationary random field is commonly used, it has been indicated that shear strength of soil in nature increase along depth with a statistically linear trend as the result of the effective overburden pressure.

There are three different types of spatial variability of a soil parameter varying with depth. Type 1: the mean and standard deviation are constants and independent of depth, i.e., the spatial

variability that can be described by the stationary random field. Type 2: the mean value increases linearly with depth but its standard deviation is independent of depth. Type 3: both the mean and standard deviation increase linearly with depth. Some studies have considered type 3 to represent the undrained shear strength of actual soil (Li et al., 2015). In our study, the spatial variability of soil strength in type 3 is simulated with a non-stationary random field as

$$H_{cu} = H_{cu0} \frac{\mu_{cu0} + kz}{\mu_{cu0}} \qquad (6)$$

where H_{cu0} is a stationary random field that is discretized with the mean and standard deviation of the shear strength at the seabed surface, i.e., μ_{cu0} and σ_{cu0}. The non-stationary random field H_{cu} is adjusted by a multiplicative scaling factor that is a function of z. In this case, the mean and standard deviation of the shear strength both increase with depth z as

$$\begin{cases} \mu_{cu}(z) = \mu_{cu0} + kz \\ \sigma_{cu}(z) = \sigma_{cu0} + \dfrac{\sigma_{cu0}}{\mu_{cu0}} kz \end{cases} \qquad (7)$$

while the coefficient of variation (COV) of the undrained shear strength is spatially constant (COV$_{cu}$ = COV$_{cu0}$ = σ_{cu0} / μ_{cu0}).

3. GPR-based surrogate model

In our study, a GPR-based surrogate model is proposed for the reliability analysis to reduce the number of direct slope stability evaluations in the MCS. The GPR method is one of the most advantageous tools among Bayesian methods. The surrogate model is built using a set of training data. The training set including a multi-dimensional input vector x_i and the corresponding output y_i. The GPR algorithm obtains the relationship between the input and output of the training database, whereupon the distribution of the predictive function $f^*(x_i)$ is provided. Then the predicted output y^* can be obtained with high accuracy given a new input x^*.

A schematic of GPR is shown in Fig. 1. With the mean function $M(x)$ and Kernel function $K(x, x')$, a Gaussian process function $f(x)$ can be specified completely as:

$$f(x) \sim GP(M(x), K(x, x')) \qquad (8)$$

where

$$\begin{cases} M(x) = E(f(x)) \\ K(x, x') = Cov(f(x), f(x')) \end{cases} \qquad (9)$$

The joint distribution of the training outputs and the predicted outputs under the prior can be expressed as

$$\begin{bmatrix} y \\ y^* \end{bmatrix} \sim N\left(0, \begin{bmatrix} K(X, X) + \sigma_n^2 I & K(X, X^*) \\ K(X^*, X) & K(X^*, X^*) \end{bmatrix}\right) \qquad (10)$$

Then the posterior probability with given input matrix $X^* = [x^*_1, x^*_2, \dots x^*_N]$ and training data is obtained based on Bayes' rule. y^* is assumed to follow the Gaussian distribution and the corresponding mean and standard deviation could be obtained.
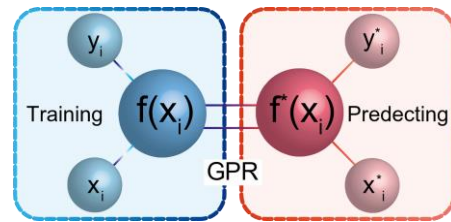

Fig. 1 Schematic of Gaussian process regression

3.1 Iterative algorithm for the surrogate model

To reduce the required number of total training samples and increase the fitting accuracy, an iterative algorithm is proposed for updating the response surface dynamically. The key to such updating lies in finding the new training point that makes the most significant contribution to the failure probability. If we want the response surface to approximate the actual performance function well, the sampling points for training should be selected on or near the limit state hypersurface.

3.2 Verification of the GPR-based RSM

An explicitly nonlinear bivariate function is used for the verification of the GPR-based RSM in this section:

$$g(\boldsymbol{x}) = \exp(0.4x_1 + 7) - \exp(0.3x_2 + 5) - 200 \qquad (11)$$

The independent random variables x_1 and x_2 both obey a standard normal distribution. Some researchers have also studied this case using different reliability analysis methods. Kim and Na (1997) proposed an RSM involving vector projected sampling points for this case, and the result of MCS with 10^6 samplings was considered as the true value for comparison ($P_f = 3.63 \times 10^{-3}$). Kaymaz (2005) proposed a kriging-based RSM, and the result of adaptive MCS was considered as the exact solution ($P_f = 3.58 \times 10^{-3}$). Deng (2006) analyzed this problem using a radial basis function (RBF) network. Lu and Yang (2006) used an artificial neural network (ANN) to solve this problem, and the result of direct MCS was again taken as the true value ($P_f = 3.63 \times 10^{-3}$).

Direct MCS with 10^8 samplings is conducted and the result of which is taken as the benchmark in this study ($P_f = 3.62 \times 10^{-3}$). The proposed GPR-based RSM is also used to calculate the failure probability. Ten initial training points are generated as uniformly distributed random numbers. One new design point is determined and added to the training database at each iterative step. After eight steps, convergence is achieved ($|P_f(n+1) - P_f(n)| < 0.01 \times 10^{-3}$). Fig. 2 shows the surfaces of the actual performance function (transparent) and the response surface fitted by the proposed GPR method. These two surfaces almost overlap in space, and the training points added during the iteration are all either on or near the limit state function.
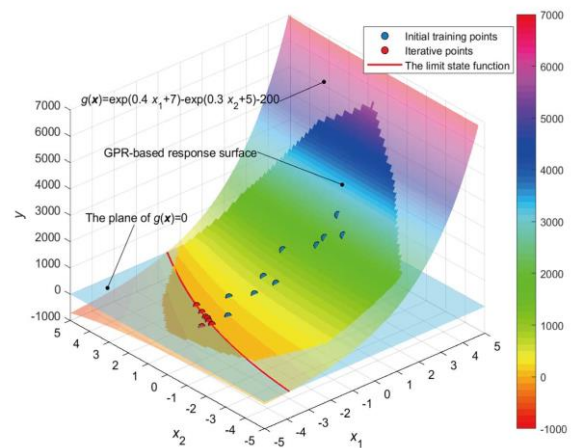

Fig. 2 Fitting results of the verification case using the GPR-based RSM with iterative algorithm

Table 1 Results of the verification case from various reliability methods

Probabilistic methods	Failure probability P_f (10^{-3})	Relative error (%)	No. of function calls	Reference
Direct MCS	3.62	-	10^8	Benchmark
Linear RSM	2.74	24.31	-	
Second-order RSM	3.45	4.70	-	Kim and Na (1997)
RSM with vector projected sampling points	3.56	1.66	31	
Second-order polynomial based RSM	3.89	7.46	-	Kaymaz (2005)
Kriging-based RSM	3.47	4.14	-	
FORM (analytical derivatives)	3.37	6.91	-	
RBF-based FORM	3.37	6.91	289	Deng (2006)
RBF-based MCS	3.84	6.08	289	
ANN-based MCS	3.67	1.38	-	Lu and Yang (2006)
GPR-based MCS	3.61	0.28	18	This study

The results of this verification case obtained from the proposed GPR-based RSM and other methods from the literature are summarized in Table 1. Only 18 function calls are needed in our study, and the result is very close to that of direct MCS with 10^8 samplings. We can see that the proposed GPR-based method in MCS has the highest efficiency and accuracy compared with other reliability methods listed in Table 1. See Zhu et al. (2019b) for more details about the GPR-base RSM.
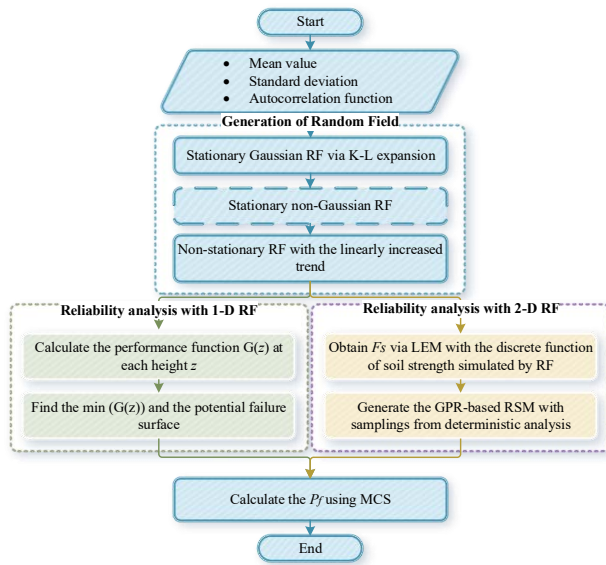

Fig. 3 Flowchart of reliability analysis of submarine slopes integrating random fields and limit equilibrium method

4. Reliability analysis of submarine slopes

Illustrative examples for both 1-D and 2-D reliability analyses of submarine slopes with spatially variable shear strength are analyzed in this section. The flowchart of the process is shown in Fig. 3. The reliability analysis consists the following steps:

(1) Generate the random field to simulate the soil strength either in the 1-D or 2-D space using the K-L expansion as described in section 2.

(2) Calculate safety factor (Fs) using the LEM combined with the random field to consider the spatial variability of soil strength.

(3) Conduct MCS to obtain the failure probability. In the two-dimensional case, the GPR-based RSM is applied to reduce the number of direct analysis of slope stability and improve the calculation efficiency.

4.1 Infinite slope model

The infinite slope model is often used when the depth of the potential failure surface is much less than the length of the slope, which is a common situation for submarine slopes. For reasons of simplicity and clarity, many studies have used the infinite slope model to evaluate the stability of submarine slopes ignoring the complexities in the analysis. However, in most studies, the spatial variability of soil parameters was not considered.

Fs of the infinite clay submarine slope model can be expressed as

$$Fs = \frac{c_u}{\gamma' z \sin\alpha \cos\alpha} \tag{12}$$

where c_u is the undrained shear strength of the marine clay which is simulated by the random field in our study. α is the slope angle and γ' is the effective unit weight of the soil. In the traditional LEM for an infinite slope model, the depth z of the slip surface is always predetermined. However, in the present study combining the LEM with random fields, the potential slip surface is located by seeking the position at which *Fs* achieves its minimum.

The thickness of marine sediments is set to 30 m in this case study. The slope angle and the effective unit weight in Eq. (12) are set to $\alpha = 5°$ and $\gamma' = 7$ kN/m^3, respectively. The unit weight of soil is treated as a constant value, because its COV is generally less than 0.1 (Phoon and Kulhawy, 1999). All three types of shear-strength described in Section 2.3 are simulated by 1-D random fields. For the stationary random field described by type 1, μ_{cu} and σ_{cu} are set to 30 kPa and 6 kPa, respectively. For the non-stationary random fields, the rate of increase of the shear strength with depth is set to $k = 1$. In type 2, namely the non-stationary random field with constant standard deviation with depth, the statistical parameters of the random field are set to $\mu_{cu0} = 15$ kPa and $\sigma_{cu} = 6$ kPa. In type 3, namely the non-stationary random field with increasing

standard deviation, the statistical parameters are set to $\mu_{cu0} = 15$ kPa and $\sigma_{cu0} = 3$ kPa, making the COV of c_u a constant and equal to 0.2, which is the same as in type 1. In the 1-D random fields, the sediment is discretized into 600 strips in the depth direction and the autocorrelation length is set to $l_v = 0.3$ m. The Gaussian random fields are used in this case study. One generation of each of these three types of random fields is shown in Fig. 4.
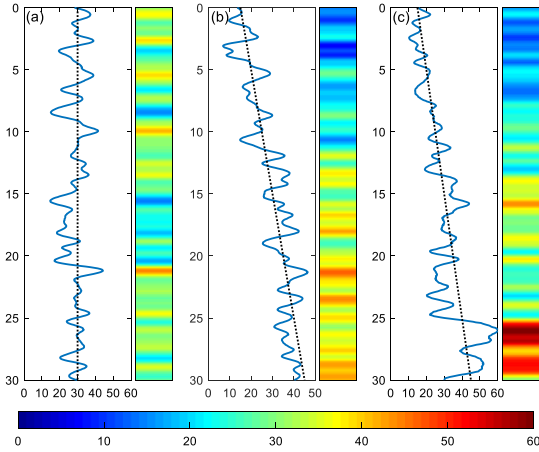

Fig. 4 One simulation of undrained shear strength of marine sediments using three types of one-D random fields

The statistics of the slip-surface depths obtained by MCS using the three types of random fields are shown in Fig. 5. If the shear strength is independent of depth as in type 1, then clearly the failure surface is most likely to be located at the bottom of the sediments, which is determined by Eq. (12): if c_u is independent of depth, then Fs is inversely proportional to depth. However, this phenomenon is alleviated in types 2 and 3 because the shear strengths increase with depth. In addition, the distribution of the failure surface is more even in type 2 than in type 3.

We then changed the correlation distance in the vertical direction in each case to study how it affects the probability of submarine slope failure. The results are shown in Fig. 6. In all three cases, probability of failure (P_f) clearly decreases with the correlation distance and converges to a certain value. The failure probability is overestimated if the linearly increasing trend of shear strength is ignored, and it is more conservative for the stability evaluation using the random field in type 2 than in type 3.
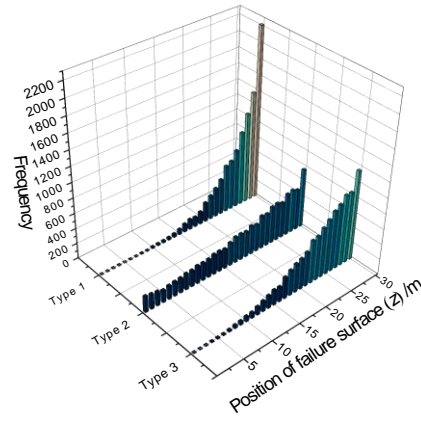

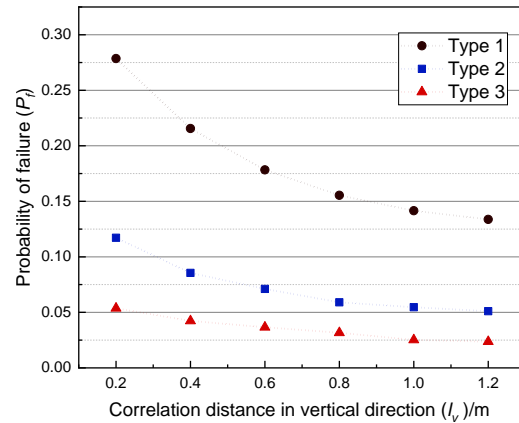Fig. 5 Histograms of positions of failure surface using three types of random fields

Fig. 6 Failure probabilities with different vertical correlation distances using three types of random fields

4.2 Two-dimensional slope model

The analysis of a simplified 2-D submarine slope with a non-stationary random field is conducted in this section. The basic parameters of this example are listed in Table 2. In this submarine slope case, the squared exponential autocorrelation function is used and the linearly increasing trend of the undrained shear strength is simulated in the random field. The distribution of the soil shear strength is set to log-normal to avoid negative values. One generation of the random field of soil strength for the two-dimensional illustrative example is shown in Fig. 7. After generating the random field, we combine it with the traditional LEM using simplified Bishop method to evaluate

the stability of submarine slope with consideration of the spatial variability of the soil shear strength.

Table 2 Parameters used in the two-dimensional submarine slope case study

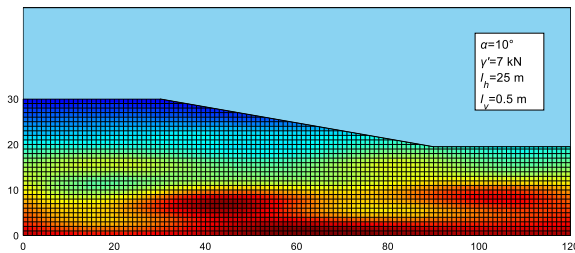| Parameter	Value	Unit
l_h	25	m
l_v	0.5	m
α	10	°
μ_{cu0}	2	kPa
Cov_{cu}	0.5	-
k	0.7	-

Fig. 7 Geometric illustration and one simulation of the random filed of the linearly increased soil shear strength for the submarine slope

For submarine slopes with gentle slope angle, the probabilities of instability are often very small. In this case, the tremendous computing workload makes it extremely difficult to use direct MCS, because a large sampling amount is needed to attain accurate results. Therefore, the proposed GPR-based RSM has shown superiority and potential in the reliability analysis of submarine slope.

The Fs values of the training samplings obtained from the surrogate model and the actual LEM analysis of the submarine slope are plotted in Fig. 8. The goodness of fit is $R^2 = 0.9405$, which indicates that the approximation accuracy of the GPR-based RSM is reasonably high. Iteration is used to find new training points closest to the limit state hypersurface. The added training points in the iteration are also plotted in Fig. 8. The histogram and cumulative distribution function (CDF) curve of Fs obtained from the MCS with GPR-based RSM are shown in Fig. 9. The distribution of P_f is close to a normal distribution. The failure probability of this case obtained from the reliability analysis is P_f

= 0.93%, and the COV of P_f is 0.0103. For more details about the reliability analysis of submarine slopes considering the spatial variability of soil strength, please refer to Zhu et al. (2019a).
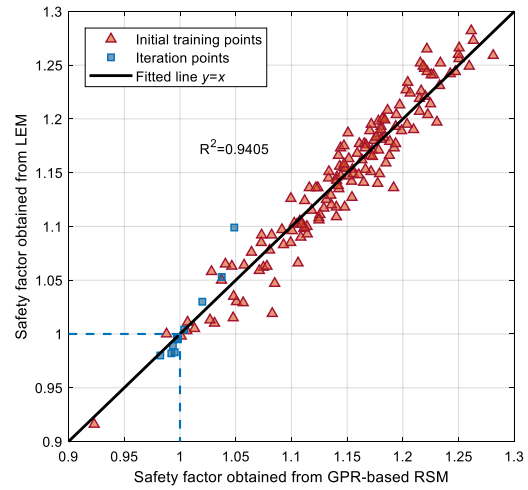

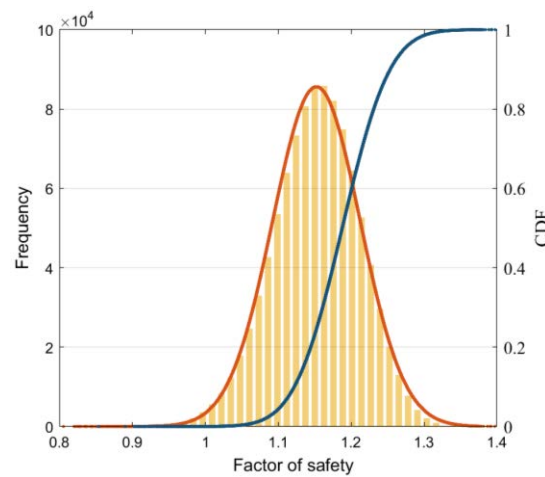Fig. 8 Approximation accuracy of the GPR-based RSM

Fig. 9 Frequency and cumulative distribution function (CDF) of Fs obtained from MCS

5. Conclusions

In this study, the reliability analysis was performed to evaluate the stability of submarine slopes using the LEM coupled with random fields both in one-D and two-D spaces. The GPR-based surrogate model was used in MCS for the complicated implicit performance function in slope stability analysis. Therefore, computation associated with the analysis is decreased. The

following conclusions are drawn based on our study.

(1) The spatial variability of sediment shear strength, which is commonly ignored in the traditional analysis of submarine slope, has a significant effect on the result of the stability evaluation.

(2) The failure probability of the submarine slope decreases with the vertical correlation distance and tends to converge to a certain value in the infinite slope model.

(3) The computational efficiency is significantly increased by incorporating the GPR-based surrogate model into the MCS. Therefore, the proposed GPR-based method has shown superiority and potential in the reliability analysis of submarine slope.

(4) Random finite element method which integrates the random field theory and finite element model will be applied to the stability analysis of submarine slopes for more complicated cases in our future study.

Acknowledgements

References

Cho, S.E. (2010): Probabilistic assessment of slope stability that considers the spatial variability of soil properties, *J. Geotech. Geoenviron. Eng*, Vol. 136, pp. 975-984.

Deng, J. (2006): Structural reliability analysis for implicit performance function using radial basis function network, *Int. J. Solids Struct.*, Vol. 43, No. 11-12, pp. 3255-3291.

Kaymaz, I. (2005): Application of kriging method to structural reliability problems, *Struct. Saf.*, Vol. 27, No. 2, pp. 133-151.

Kim, S.H. and Na, S.W. (1997): Response surface method using vector projected sampling points, *Struct. Saf.*, Vol. 19, No. 1, pp. 3-19.

Lacasse, S. and Nadim, F. (1996): Uncertainties in characterising soil properties, *Geotechnical Engineering-division Specialty Conference on Uncertainty in the Geologic Environment - From Theory to Practice*, ASCE, pp. 49-75.

Li, D.Q., Qi, X.H., Cao, Z.J., Tang, X.S., Zhou, W., Phoon, K.K., and Zhou, C.B. (2015): Reliability analysis of strip footing considering spatially variable undrained shear strength that linearly increases with depth, *Soils Found.*, Vol. 55, pp. 866-880.

Lu, Z. and Yang, Z. (2006): New reliability analysis method based on artificial neural network, *J. Mech. Strength*, Vol. 28, No. 5, pp. 699-702.

Phoon, K.K. and Kulhawy, F.H. (1999): Characterization of geotechnical variability, *Can. Geotech. J.*, Vol. 36, pp. 612-624.

Yang, S., Nadim, F., and Forsberg, C.F. (2007): Probability study on submarine slope stability, in: Lykousis, V., Sakellariou, D., and Locat, J. (Eds.), *Advances in Natural and Technological Hazards Research*, Springer, pp. 161-170.

Zhu, B., Pei, H., and Yang, Q. (2018): Probability analysis of submarine landslides based on the response surface method: a case study from the South China Sea, *Appl. Ocean Res.*, Vol. 78, pp. 167-179.

Zhu, B., Pei, H., and Yang, Q. (2019a): Reliability analysis of submarine slope considering the spatial variability of the sediment strength using random fields, *Appl. Ocean Res.*, Vol, 86, pp. 340-350.

Zhu, B., Pei, H., and Yang, Q. (2019b): An intelligent response surface method for analyzing slope reliability based on Gaussian process regression, *Int. J. Numer. Anal. Methods Geomech.*, Vol. 43, pp. 2431-2448.

(Received July 2, 2020)